

Three Type I X-ray bursts from Cyg X-2: Application of Analytical Models for Neutron Star Mass and Radius Determination

Lev Titarchuk¹, and Nickolai Shaposhnikov²

ABSTRACT

We study the spectral and temporal properties of three Type I X-ray bursts observed from Cyg X-2 with *the Rossi X-ray Timing Explorer*. Despite the short time durations (~ 5 sec) these bursts show radial expansion of order of several neutron star (NS) radii. We apply the analytical models of spectral formation during the expansion and contraction stages to derive physical conditions for the matter in the burning zone close to the surface of the NS as well as The NS's mass-radius relation. Our results, combined with statistical errors, show that the central object is a compact star with mass ~ 1.4 solar masses and radius ~ 9 km. Our results favor the softer equation of state for neutron star matter.

Subject headings: accretion—radiative transfer—stars:fundamental parameters—stars:individual(Cyg X-2)—stars:neutron—X-ray:bursts

1. Introduction

The strong energy outbursts in the atmospheres of neutron stars in low mass X-ray binary (LMXB) systems are commonly referred to as X-ray bursts. Soon after their discovery by Grindlay & Heise (1975), X-ray bursts were separated into two classes: in Type I and Type II bursts. Type I bursts are currently considered to be due to thermonuclear explosions on a neutron star (NS) surface, and Type II bursts are believed to result from the instability of the gravitational energy release in the accretion flow (see Lewin et al. 1993). Very strong Type I bursts (hereafter bursts, unless otherwise stated) can exhibit radial atmospheric

¹George Mason University/Center for Earth Observing and Space Research, Fairfax, VA 22030; and US Naval Research Laboratory, Code 7620, Washington, DC 20375-5352; lev@xip.nrl.navy.mil

²George Mason University, School for Computational Sciences; Center for Earth Observing and Space Research, Fairfax, VA 22030; nshaposh@scs.gmu.edu

expansion. After the burst’s peak, when the luminosity falls below the Eddington limit, the atmosphere quickly contracts back to the NS surface.

Titarchuk (1994a) (hereafter T94) and Shaposhnikov & Titarchuk (2002) (hereafter ST02) developed the analytical theory of spectral formation during the expansion and contraction stages of the burst. Two cases have to be considered separately when the Eddington ratio $l = L/L_{\text{Edd}} \sim 1$ and when $l < 0.9$ (i.e., before and after the “touchdown” of the extended atmosphere). In the former case, the radiation pressure has substantial influence on the NS atmosphere dynamics, while in the latter one can utilize the hydrostatic equilibrium approximation. The T94 theory can be used to derive distances to X-ray burst sources from which only burst luminosities below the Eddington limit are observed. Haberl & Titarchuk (1995) (hereafter HT95) applied the T94 theory to 4U 1705-44 and they found a distance 7.4 ± 1 kpc, assuming similar NS mass-radius relation for 4U 1705-44 and 4U 1820-30. HT95 presented constraints on the NS mass-radius relationship in X-ray burst source 4U 1820-30. We extend this methodology by deriving the temperature of the burning zone and applying the theory of spectral formation during the expansion stage to the observational spectra obtained at the peaks of bursts. We show that when the mass-radius contours obtained by applying this theory to observations are combined with the Eddington limit constraints for peak flux, we obtain separate NS mass and NS radius values.

Most X-ray bursts are observed in LMXB sources whose color-color diagrams cause them to be classified as atoll sources. However, the two Z-sources GX 17+2 and Cyg X-2 are exceptions to this rule. The observational data of X-ray missions prior to RXTE suffered from poor statistical and time resolution properties and thus could not resolve the nature of burst-like events detected from these sources. The first incontestable evidence of a Type I burst from Cyg X-2 was reported by Smale (1998) (hereafter S98). The analysis provided by S98 indicates that the burst color temperature increases with the transition to the contraction stage and it goes down during a burst decay. In this *Letter* we concentrate our efforts on the study of the spectral properties of the bursts from the source Cyg X-2. We have surveyed the RXTE public data archive and find more than 20 burst events where the count rate increased by a factor of three on a time scale of $1 \sim 2$ seconds. Temporal analysis of this set of bursts for which appropriate data configurations are available shows that for only three bursts (including the burst reported by S98) can the photospheric radius expansion be well established. As long as no other burst can be qualified as a Type I, we summarize the results provided by the three bursts with radial expansion. In §2 we present the results of the analytical models for X-ray spectral formation in the burst atmospheres along with the methodology which we implement in our data analysis. §3 describes the observational data and reduction procedure. §4 contains a report of our results, which is followed by discussion and conclusions in §5.

2. Models for a spectral formation during expansion and contraction stages

T94 presented analytical approximations for the solution of the radiative transfer problem during the burst, covering a wide range of values for the Eddington ratio l . In a case of the hydrostatic equilibrium atmosphere ($l < 0.9$) the density profile is exponential. The solution for the color factor T_h as a function of the luminosity l , the helium abundance Y_{He} , and the gravitational acceleration g is obtained in the form (T94)

$$T_h = T/T_{eff} = 1.32K(l, Y_{He}, g)\Lambda_*^{-4/5}, \quad (1)$$

where

$$K(l, Y_{He}, g) = l^{3/20}(1 - 5Y_{He}/8)^{2/15}(1 - Y_{He}/2)^{-1/60}(1 - l)^{-2/15}g_{14}^{1/60},$$

$$\Lambda_* = 0.14 \ln(8a) + 0.1 \exp(-5.5a) + 0.6, \quad a = K^{15/2}(l, Y_{He}, g) \text{ and } g_{14} = g/10^{14} \text{ cm s}^{-2}.$$

The radiative transfer equation in the $l \sim 1$ case also admits a semi-analytical treatment, which is presented in detail in ST02. Here we present the final results, obtained for the color factor T_h and color temperature kT

$$T_h = 0.37 m^{0.174} r_6^{-0.28} T_{b,9}^{-0.64} (2 - Y_{He})^{-0.074}, \quad (2)$$

$$kT = 0.76 m^{0.42} r_6^{-0.78} T_{b,9}^{-0.64} (2 - Y_{He})^{-0.324} \text{ keV}, \quad (3)$$

where r_6 is the NS radius in units of 10^6 cm, $m = M_{NS}/M_\odot$ is the NS mass in units of the solar mass, and $T_{b,9}$ is the temperature at the bottom of the burst atmosphere in units of 10^9 K. With these expressions in hand (Eqs. 1-3), we apply our formalism to PCA burst data. The outcome of the fitting procedure implemented to X-ray burst data are the color temperature of radiation kT_∞ and the bolometric flux F_b with corresponding statistical errors. Subscripts ∞ and b denote the fact that these values are detected by a distant observer. Renormalization to the real condition at the photospheric surface should account for both dilution and gravitational redshift. The dilution is described by the relation $L_\infty = 4\pi d^2 \xi_b F_b$, where ξ_b is the anisotropy factor determined by the emission anisotropy of the burst. The local luminosity L and temperature kT are connected with those observed at infinity by

$$L_\infty = L/(z + 1)^2, \text{ and } kT_\infty = kT/(z + 1), \quad (4)$$

where the redshift factor is $(z + 1) = (1 - 2GM_{NS}/R_{NS}c^2)^{-1/2} = (1 - 0.297m/r_6)^{-1/2}$.

From the definition of the effective temperature and color factor we can write

$$4\pi R_{NS}^2 \sigma T_{eff}^4 = 4\pi R_{NS}^2 \sigma (T/T_h)^4 = L. \quad (5)$$

After the atmospheric “touchdown” occurs (or when no substantial photospheric expansion occurs) we rewrite L as $l L_{\text{Edd}}$, where

$$L_{\text{Edd}} = 4\pi c G M_{\text{NS}}(z+1)/\kappa_0(2 - Y_{\text{He}}) = L_{\text{Edd},\infty}(z+1), \quad (6)$$

with $\kappa_0 = 0.2 \text{ cm}^2\text{g}^{-1}$. Substituting this into (5), after introducing the general relativistic corrections in (4), we obtain

$$r_6^2 = 19.5(T_h/kT_\infty)^4 l m / (2 - Y_{\text{He}})(z+1)^3. \quad (7)$$

The dimensionless luminosity l measured by a local observer can be expressed in terms of observed fluxes and gravitational redshift as

$$l = L/L_{\text{Edd}} = F_b(z+1)/F_{b,\text{Edd}}, \quad (8)$$

where $F_{b,\text{Edd}} \approx L_{\text{Edd},\infty}/(4\pi d^2 \xi_b)$ is the observed burst peak bolometric flux (we neglect the relativistic corrections in evaluating $F_{b,\text{Edd}}$). Using the above expression for $F_{b,\text{Edd}}$ and Eq. (6) for $L_{\text{Edd},\infty}$, we can rewrite this equation as

$$l = 0.476 \xi_b d_{10}^2 F_{b,8} (2 - Y_{\text{He}})(z+1)/m, \quad (9)$$

where $d_{10} = d/10 \text{ kpc}$, and $F_{b,8} = F_b/10^{-8} \text{ erg cm}^{-2} \text{ s}^{-1}$. Because T_h and $z+1$ are dependent of r_6 we can find r_6 as a numerical solution of equation (7) for a particular set of the parameters m and Y_{He} . Furthermore, we can determine the NS mass m using the Eddington limit (6), provided that the distance to the source is known. Finally, we are able to test the conditions at the burning zone during the expansion stage by virtue of relation (3).

3. Observations

The Z-source Cyg X-2 has been observed extensively by the proportional array counter (PCA) onboard RXTE throughout the mission. We reviewed the entire Cyg X-2 archived data set in an attempt to locate thermonuclear bursts. When a burst was found we determined what EDS (Experimental Data System) configuration was used for that observation. We then choose those bursts for which the EDS configuration was well suited to our analysis. Among the more than 20 burst-like events, we choose three for our analysis: Burst 1 was detected on March 27, 1996 (ObsId:10066-01-01-00, S98), burst 2 was detected on August 10, 1998 (ObsId: 20046-01-05), and burst 3 was detected on September 12, 1998 (obsID: 30046-01-01-00). The first two bursts can be classified confidently as Type I X-ray bursts. The nature of burst 3 is uncertain, as we discuss below. During these observations, four additional EDS modes were utilized along with two standard modes: binned mode (0-35

PCA channels in 16 energy bins, 2 ms time resolution), event mode (36-255 PCA channels in 64 bins, 125 μs time resolution), and two single-bit modes with 125 μs time resolution, covering the 0-13 and 14-35 PCA energy channels correspondingly. Burst 1 was observed during PCA gain epoch 2, while burst 2 and 3 were observed during PCA gain epoch 3 resulting in a different instrumental response for across the PCA channels. For our temporal burst analysis we are particularly interested in binned and event modes. For the data reduction we use the procedure adopted by Smale (1998), in that we extract a sequence of 0.5 second spectral slices during each burst. Then we extract the spectra of persistent emission prior to each burst. The time duration for the persistent emission spectra is determined by the requirement that the persistent flux does not undergo substantial systematic changes during the interval. All spectra produced are dead-time corrected according to RXTE Data Reduction Recipes.

4. Data analysis and results

The best fits for persistent flux background spectra were obtained using the XSPEC comptt+bbody model (Titarchuk 1994b). Best fit parameters for bursts 1, 2, and 3 respectively are: soft photon temperature = 1.09 ± 0.06 , 1.04 ± 0.02 , 1.04 ± 0.05 keV, plasma temperature = 3.1 ± 0.1 , $4.2^{+1.2}_{-0.6}$, 3.0 ± 0.2 keV, plasma optical depth = 4.7 ± 0.3 , $2.16^{+0.45}_{-0.6}$, 3.9 ± 0.4 , black body temperature = 0.56 ± 0.03 , 0.47 ± 0.03 , 0.47 ± 0.05 keV. For each burst we fit each half-second spectral slices over the energy range 2.8-30 keV. using the black-body model which best describes the background subtracted burst emission. To obtain the burst emission we subtract the persistent component as given by analysis of preburst data. The radiated energy from the burst can affect the persistent flux both in magnitude and its spectral properties causing systematic trends in our results. Specifically, if burst results in an increase of the persistent component, our analytical approach will result in slight overestimation of the NS radius.³ The best fit values of the color temperatures kT , the reduced χ^2_{red} values of the blackbody spectral fits to the data, accompanied by the luminosities l and the inferred NS radii, are plotted on Figure 1. The typical behavior of a thermonuclear runaway process is most pronounced in the first burst: after a quick rise, the color temperature gradually hardens from 1 keV up to 2 keV and then decreases during decay phase. The situation is less obvious for burst 3, where the temperature stays rather high throughout the decay. We speculate that the persistent emission is affected by the burst itself. In fact, the photons generated by the bursts can be intercepted by the accretion disk and reflected. This results

³At this point we cannot refine the method of persistent emission subtraction due to the quality of data and the fact that no theoretical model for interaction of burst and persistent energy flux has been developed.

in apparent anisotropy of the burst radiation [see Lapidus, Sunyaev & Titarchuk (1985), Popham & Sunyaev (2001) for details].

The second burst has a peak flux, approximately 25% higher than that of the other two bursts. This discrepancy can be again explained by considering disk reflection and/or dynamical evolution of the NS - accretion disk geometry ⁴. The anisotropy effect can be accounted for in our analysis by the inclusion of the anisotropy coefficient in equation (9). Unfortunately, the limited signal-to-noise of the Cyg X-2 data during the burst decay part does not allow us to make any further conclusions on this issue. To ensure consistency with the observed peak fluxes, we set the anisotropy parameter constant to 0.8 for the second burst, while we keep it at unity for the first and the third bursts.

Combining equations (1), (7) and (9) we obtain an equation relating the NS mass and radius to quantities we can obtain from the observations:

$$r_6^2 = 9.28\xi_b d_{10}^2 F_{b,8} (T_h/kT_\infty)^4 (1 - 0.297m/r_6). \quad (10)$$

We solve equation (10) for each pair of values kT_∞ , $F_{b,8}$ and a given set of parameters Y_{He} and m to obtain the radius of the emitting surface r_6 and Eddington ratio l . It should be noted that a solution exists in the narrow parameter space for r_6 , m and Y_{He} only. In Figure 1 the values of the inferred characteristics are shown along with a plot of color temperatures, obtained using blackbody fits to the data. After the luminosity peak the photospheric radius drops quickly, while l remains close to unity. After about 4 seconds the photosphere reaches “touchdown”, the radius levels off at constant value and the Eddington ratio drops rapidly. Because the thickness of the atmosphere (scale height $H \approx kT/mg \sim 10^2$ cm) is negligible with respect to the neutron star radius R_{NS} , we assume the photospheric radius, R_{ph} after “touchdown”, is equal to the R_{NS} . Then for a particular distance we determine the NS mass assuming the Eddington luminosity at the peak of the burst. Figure 2 shows two contours for distances of 9 and 11 kpc and cosmic elemental abundance along with the R , π and π' equations of state for neutron star matter from Baym & Pethick (1979). The points with error bars on mass and radii present NS mass-radius determination. For an assumed distance of 11 kpc we obtain the canonical values for the neutron star parameters: mass = 1.44 ± 0.06 , radius = 9.0 ± 0.5 km, while assuming 9 kpc the results are less realistic: mass = 0.97 ± 0.04 , radius = 7.7 ± 0.4 km (quoted errors on the NS mass includes only the statistical error on the burst peak flux). The lack of convergence is the reason why the contour for $d = 9$ kpc ends at $m = 1.4$. If we demand that our model yields $m \approx 1.4$ and $Y_{He} \approx 0.3$ then our results

⁴The area of emitting NS surface exposed to observer can change during bursts with radial expansion. A strong indication that this may occur has recently been found by the authors in X-ray bursts from 4U 1728-34. We will discuss this point in a forthcoming paper.

favor the soft, specifically R and π , equations of states for neutron stars. Using formula (3) we estimate the burning zone temperature at the maximum expansion is within the range $(4 - 6)10^8$ K.

5. Discussion and Conclusions

In light of the recently discovered millisecond variability in the X-ray flux from a number of LMXBs, the task of independent determination of masses and radii of neutron stars in these systems becomes very important. Kilohertz Quasi-periodic oscillations (QPO) are seen in the power-density spectrum of many LMXBs as twin peaks with frequencies within the range of 500-1200 Hz. A number of models were put forward to explain these high-frequency patterns. First, and most obvious, was the suggestion of an interaction between Keplerian frequency at neutron star surface (or last stable orbit) and the frequency of the neutron star rotation [beat-frequency model (BFM): Alpar & Shaham (1985); Miller Lamb & Psaltis (1998)]. Despite some discrepancies between the model predictions and the observational results, [the peak separation is not constant when the twin QPO frequencies vary with time (see e.g. van der Klis 2000)], the beat-frequency model became fashionable and has been applied to infer information on the neutron star masses Zhang et al. (1997). Because of general relativistic (GR) effects, no stable particle motion is allowed for a circular orbit radius less than $R_{isco} = 6GM/c^2 = 8.9m$ km. The corresponding frequency of the orbital motion (assumed close to the QPO frequency) is $\nu_{isco} \approx 2210/m$ Hz. The NS masses in the LMXB exhibiting kHz QPO phenomena should be equal to or even exceed two solar masses if the highest observed kHz QPO is interpreted as the frequency of the innermost stable orbit. For Cyg X-2 the corresponding values are 1005 Hz for the maximum QPO frequency (Wijnands & van der Klis 1998) and consequently $2.2M_{\odot}$ is the NS inferred mass, clearly too high. *Our analysis of the burst spectra, which takes into account all corrections due to the GR and electron scattering effects, are in disagreement with the mass-radius constraints obtained using the kHz QPO frequencies values evaluated within the BFM frameworks.*

It is worth noting that in a recent study of optical and UV lightcurves of Cyg X-2 by Orosz & Kuulkers (1999) who elaborate independent constraints on the NS mass in Cyg X-2, they find $M_{NS} = 1.78 \pm 0.23 M_{\odot}$, consistent with our mass determination above ⁵.

⁵There remains the problem of the too small distance estimates of $d_{10} = 0.72 \pm 0.11$ obtained by Orosz & Kuulkers (1999). But this can be explained as the uncertainty in the luminosity estimate for Cyg X-2 optical counterpart, caused by an unknown disk contribution. We should emphasize that the X-ray radiation detected from a type I burst is directly related to the physical processes (thermonuclear explosions, photon transport) which take place in the NS atmosphere. Consequently it carries with it direct information

Sco X-1 and Cyg X-2 have many similar features in terms of their timing and spectral properties and they have almost the same upper limit for the bolometric flux (see Bradshaw, Fomalont & Geldzahler, 1999). Thus we expect that the similar mass-radius values inferred for Cyg-2 (mass = 1.44 ± 0.06 , radius = 9.0 ± 0.5 km) should also be applied to Sco X-1.

The authors are grateful to Menas Kafatos for support of this work and to the referee for fruitful suggestions. We acknowledge the thorough analysis and editing of the paper by Michael Wolff.

REFERENCES

- Alpar, M. A., & Shaham, J. 1985 , Nature, 316, 239
- Baym, G., & Pethick, C. 1979, Ann. Rev. Astr. Ap. 17, 415
- Bradshaw, C. F., Fomalont, E. B., & Geldzahler, B. J. 1999, ApJ, 512, L121
- Grindlay, J. E., & Heise, J. 1975, IAU Circ.2879
- Haberl, F., & Titarchuk L. 1995, A&A, 299, 414 (HT95)
- Lapidus, I. I., Sunyaev, R. A., & Titarchuk, L. G. 1985, Astrophysics, 23, 3, 663
- Lewin, W.H. G., van Paradijs, J., & Taam, R. E. 1993, Space Sci. Rev., 62, 223
- Miller, M. C., Lamb, F. K., & Psaltis, D. 1998, ApJ, 508, 791
- Orosz, J. A., Kuulkers, E. 1999, MNRAS, 305, 132
- Popham, R., & Sunyaev, R. 2001, ApJ, 547, 355
- Smale, A.P. 1998, ApJ, 498, L41
- Shaposhnikov, N., & Titarchuk, L. 2002, ApJ, 567, 1077 (ST02)
- Titarchuk, L. 1994a, ApJ, 429, 330 (T94)
- Titarchuk, L. 1994b, ApJ, 434, 570
- Zhang, W., Strohmayer, T. E., & Swank, J. H. 1997, ApJ, 482, L167

regarding the main NS characteristics (mass, radius) and the distance to the source.

van der Klis M. 2000, ARA&A, 38, 717

Wijnands R., & van der Klis M. 1998, IAU Circ.6876

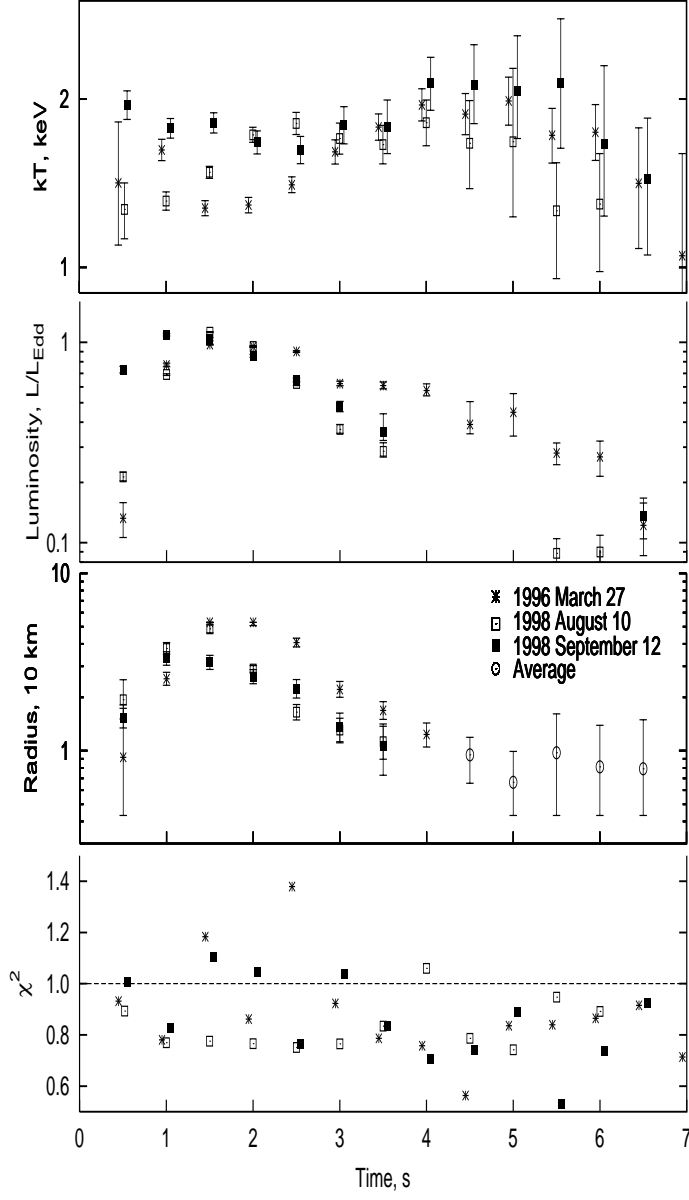


Fig. 1.— Time dependence of the inferred photospheric radius, dimensionless luminosity l , the color temperature and χ^2_{red} values of the spectral fits from our analysis for input parameters $Y_{He} = 0.3$, distance = 10 kpc, and a neutron star of 1.44 solar mass. The observed flux for 1998 September 12 was renormalized in the analysis by a factor of 0.8 (see text).

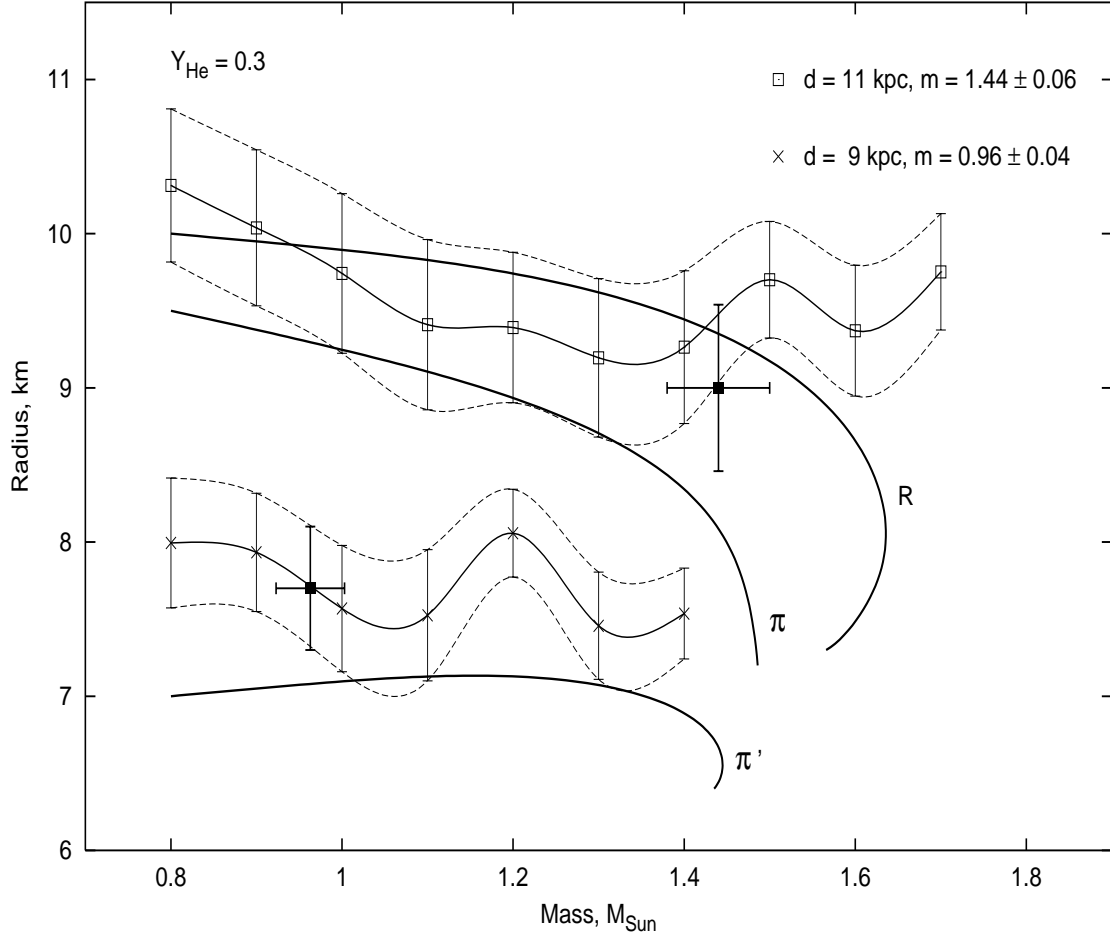


Fig. 2.— Regions of the NS mass-radius parameter space admitted by the burst model for the cosmic helium abundance. The upper region is assuming a distance of 11 kpc and the low region has a distance 9 kpc. The width of each region is a function of the observational errors in flux $F_{b,8}$ and kT_{∞} . The two points with error bars on mass and radius represent the mass-radius determinations inferred from the average peak (Eddington) luminosity and the contraction stage spectra.